

# MODEL-BASED FLAW RECONSTRUCTION AND FLAW PARAMETER ESTIMATION USING A LIMITED SET OF RADIOGRAPHIC PROJECTIONS

Richard M. Wallingford and John P. Basart

Dept. of Electrical and Computer Engineering  
Center for Nondestructive Evaluation  
Iowa State University  
Ames, IA 50011

## INTRODUCTION

This paper presents an approach to the reconstruction and parameter estimation of flaw models in NDE radiography. The reconstruction of flaw models rather than the flaw distribution itself reduces the required number of projections as well as the complexity of the measurement system [1,2]. In this approach, crack-like flaws are modeled as piecewise linear curves, and volumetric flaws are modeled as ellipsoids. Our emphasis here is on a method for estimating the model parameters for crack-like flaws using a linear model with more than the minimal number of required projections. Extra projections reduce the effects of measurement errors and film noise. We also present the development of the volumetric flaw model and outline a method for its inversion.

## PARAMETER ESTIMATION FOR CRACK-LIKE FLAWS

We have shown previously [1] that two projections using a linear sample shift is the minimum number required for a unique solution of the model parameters. With two projections, there are 10 governing equations, 6 unknown desired parameters, and two unknown nuisance parameters. We therefore have an overdetermined linear system of equations with many possible solutions due to random fluctuations in the measurement variables. The linear model describing the crack-like flaw is given by Equation (1).

$$\mathbf{R} = \mathbf{H} \Theta \tag{1}$$

$$\mathbf{R} = \begin{bmatrix} (\mathbf{V}_{3x} - \mathbf{V}_{1x}) - \Delta x \\ \mathbf{V}_{1y} - \mathbf{V}_{3y} \\ (\mathbf{V}_{4x} - \mathbf{V}_{2x}) - \Delta x \\ \mathbf{V}_{2y} - \mathbf{V}_{4y} \\ \mathbf{V}_{1x} \\ \mathbf{V}_{1y} \\ 0 \\ \mathbf{V}_{2x} \\ \mathbf{V}_{2y} \\ 0 \\ \cdot \\ \cdot \end{bmatrix} \quad \Theta = \begin{bmatrix} t_1 \\ t_2 \\ \mathbf{V}_{c1x} \\ \mathbf{V}_{c1y} \\ \mathbf{V}_{c1z} \\ \mathbf{V}_{c2x} \\ \mathbf{V}_{c2y} \\ \mathbf{V}_{c2z} \end{bmatrix}$$

$$\mathbf{H} = \begin{bmatrix} \mathbf{V}_{1x} - \mathbf{V}_{3x} & 0 & 0 & 0 & 0 & 0 & 0 & 0 \\ \mathbf{V}_{1y} - \mathbf{V}_{3y} & 0 & 0 & 0 & 0 & 0 & 0 & 0 \\ 0 & \mathbf{V}_{2x} - \mathbf{V}_{4x} & 0 & 0 & 0 & 0 & 0 & 0 \\ 0 & \mathbf{V}_{2y} - \mathbf{V}_{4y} & 0 & 0 & 0 & 0 & 0 & 0 \\ \mathbf{V}_{1x} - \mathbf{V}_{1x} & 0 & 1 & 0 & 0 & 0 & 0 & 0 \\ \mathbf{V}_{1y} - \mathbf{V}_{1y} & 0 & 0 & 1 & 0 & 0 & 0 & 0 \\ -\mathbf{V}_{1z} & 0 & 0 & 0 & 1 & 0 & 0 & 0 \\ 0 & \mathbf{V}_{2x} - \mathbf{V}_{2x} & 0 & 0 & 0 & 1 & 0 & 0 \\ 0 & \mathbf{V}_{2y} - \mathbf{V}_{2y} & 0 & 0 & 0 & 0 & 1 & 0 \\ 0 & -\mathbf{V}_{2z} & 0 & 0 & 0 & 0 & 0 & 1 \\ \cdot & & & & & & & \\ \cdot & & & & & & & \end{bmatrix}$$

The linear model comes about through the system of parameterized vector equations describing the x-ray path through the endpoints of the crack. The generic form of the vector equation is given by

$$\mathbf{V}_i = \mathbf{V}_d - t_i (\mathbf{V}_s - \mathbf{V}_d) , \tag{2}$$

where  $\mathbf{V}_i$  is the vector from the origin to the projection of the  $i$ th crack endpoint in the detector plane,  $\mathbf{V}_d$  is the vector to the  $i$ th crack endpoint in 3-D,  $\mathbf{V}_s$  is the vector to the x-ray microfocus x-ray source, and  $t_i$  is a parameter. Since any linear segment of a crack has two projected end points, there are four crack endpoints for two projections. In the linear model above,  $\mathbf{V}_{1x}$ ,  $\mathbf{V}_{1y}$ ,  $\mathbf{V}_{2x}$ , and  $\mathbf{V}_{2y}$  represent the x and y components of the vector to the

two crack endpoints in the detector plane with the first projection. The quantities  $V_{3x}$ ,  $V_{3y}$ ,  $V_{4x}$ , and  $V_{4y}$  represent the x and y components of the vector to the two crack endpoints in the detector plane with the second projection. Note that the subscripts 1 and 3 correspond to the same crack endpoint as well as subscripts 2 and 4.  $\Delta x$  is the distance the sample is translated in the x direction for the second projection.  $V_{sx}$ ,  $V_{sy}$ , and  $V_{sz}$  are the x, y, and z components of  $V_s$  in (2). The elements of the parameter vector,  $V_{c1x}$ ,  $V_{c1y}$ ,  $V_{c1z}$ ,  $V_{c2x}$ ,  $V_{c2y}$ , and  $V_{c2z}$  are the components of  $V_{ci}$  in (2);  $t_1$  and  $t_2$  are the nuisance parameters for the first and second projection respectively.

Notice that the explanatory variables in the model matrix,  $H$ , include measurement variables. In this situation, errors in the explanatory variables must be allowed in the parameter estimator. A method which arrives at an optimal solution for the parameter vector in the sense of minimum squared error is the method of total least-squares (TLS). This method is similar to the method of ordinary least squares except that it allows for errors in the model itself. In TLS, the error is measured as a distance orthogonal to the solution hyperplane rather than orthogonal to the hyperplane defined by the explanatory variables. An illustration of the error criterion for the 2-D case is shown in Fig. 1.

The TLS solution can be computed by different methods. One method, developed by Golub and Van Loan [3], uses the singular value decomposition (SVD) of the model matrix augmented by the measurement vector. The SVD, given by Equation (3), consists of an ( $m \times m$ ) orthogonal matrix  $U$ , the ( $m \times n+1$ ) matrix of singular values  $\Sigma$ , and an ( $n+1 \times n+1$ ) orthogonal matrix  $V^T$  where super T indicates the transpose.

$$C = [H \mid R] = U \Sigma V^T \quad (3)$$

The solution to the TLS problem is obtained from the minimum right singular vector. This vector is the column of  $V^T$  corresponding to the minimum singular value in  $\Sigma$ . The optimal solution vector,  $\theta_{opt}$ , is the first n components of the minimum right singular vector normalized by the negative of the ( $n+1$ )st component of the vector. The TLS solution is not guaranteed to exist unless the minimum singular value associated with  $H$  is less than that of  $[H \mid R]$ .

A second method for the TLS solution uses the normal equations [4]. The normal equations are the set of equations obtained by minimizing the residual error with respect to each parameter. In this case, the optimal parameter vector is given by

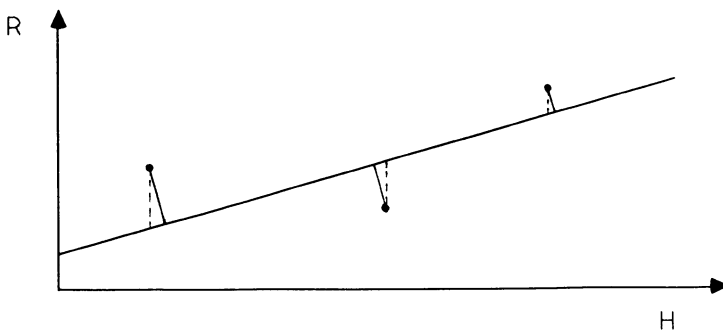


Figure 1. Ordinary least squares versus total least squares.

$$\theta_{\text{opt}} = \left( \mathbf{H}^T \cdot \mathbf{H} - s_{n+1}^2 \mathbf{I} \right)^{-1} \mathbf{H}^T \mathbf{R}. \quad (4)$$

The square of the minimum singular value,  $s_{n+1}^2$  can be computed from an eigenvalue-eigen vector decomposition rather than an SVD with this technique.

The main trade-off between these two techniques is speed and storage space versus algorithm stability. The SVD is more stable than the normal equations [5], but the normal equation method can be programmed for faster execution and less storage space [4].

The advantage of using a least-squares estimator over using eight of the model equations to solve for the eight unknowns is that it allows data from multiple projections (more than two) to be used to better estimate the parameters. The linear system given in (1) can be augmented with many more rows to accommodate the extra projections.

### VOLUMETRIC FLAW RECONSTRUCTION

For reconstruction of volumetric flaws, we use an ellipsoidal solid model with arbitrary principal axes lengths, arbitrary orientation, and arbitrary centroid location. With these quantities as model parameters, a wide variety of shapes of flaws can be described ranging from long thin needles, to flat pancakes or void-like spheres. The technique used for reconstructing such a model is to formulate the theoretical forward projection model and use measured projection data to invert the model equations and solve for the model parameters.

The forward projection model for the ellipsoid is essentially its Radon transform. The general 3-D Radon transform for an arbitrary object function is given by

$$\mathbf{R}[f(\mathbf{x})] = g(s, \alpha) = \iiint f(\mathbf{x}) \delta(\mathbf{x}^T \alpha - s) d\mathbf{x} \quad (5)$$

The x-ray intensity at any point on the detector plane is proportional to the line integral of the object function along the line connecting the source to the detector. Thus, the collection of intensities on the detector plane constitutes the Radon transform of the object for the particular detector orientation.

For a parallel beam x-ray source, we can derive an analytic expression for the Radon transform of the ellipsoidal function. The ellipsoidal function is given by

$$f(x,y,z) = \begin{cases} 1 & \frac{x^2}{A^2} + \frac{y^2}{B^2} + \frac{z^2}{C^2} \leq 1 \\ 0 & \text{elsewhere} \end{cases}, \quad (6)$$

where  $x, y, z$  are the cartesian coordinates, and  $A, B, C$  are the semi-lengths of the ellipsoidal axes along the coordinates respectively. The function does not assume any rotation or translation as this will be accommodated in the rotational and translational properties of the Radon transform. By computing the distance between intersection points of an x-ray line and the ellipsoidal surface, the Radon transform can be derived.

We define the detector plane by the (r,t) coordinate axes that correspond to the (z,x) axes in the unrotated coordinate system. Using parallel beam geometry, the line describing the x-ray path impinging on point  $(r_o, t_o)$  in the detector plane is given by the intersection of the two planes,

$$\begin{aligned} r &= r_o \\ t &= t_o \end{aligned}$$

We now allow for the rotation of the detector plane by the three angles  $\theta$ ,  $\gamma$  and  $\psi$ . The angle  $\theta$  is a rotation counterclockwise about the z axis in a right-hand coordinate system, the angle  $\gamma$  is a rotation about the new x axis (after the  $\theta$  rotation), and the angle  $\psi$  is a rotation about the new y axis (after both  $\theta$  and  $\gamma$  rotations). The transformation matrix for this rotation is

$$\begin{bmatrix} \cos \psi \cos \theta - \sin \psi \cos \gamma \sin \theta & \cos \psi \sin \theta + \sin \psi \cos \theta \cos \gamma & \sin \psi \sin \gamma \\ -\sin \psi \cos \theta - \cos \psi \cos \gamma \sin \theta & -\sin \psi \sin \theta + \cos \psi \cos \theta \cos \gamma & \cos \psi \sin \gamma \\ \sin \gamma \sin \theta & -\sin \gamma \cos \theta & \cos \gamma \end{bmatrix}$$

The equation for the line describing the x-ray impinging on point  $(r_o, t_o)$  in the rotated detector plane is now given by the intersection of the two planes

$$r_o = x \cdot (\sin \gamma \sin \theta) + y \cdot (-\sin \gamma \cos \theta) + z \cdot \cos \gamma \quad (7)$$

$$t_o = (\cos \psi \cos \theta - \sin \psi \cos \gamma \sin \theta) \cdot x + (\cos \psi \sin \theta + \sin \psi \cos \theta \cos \gamma) \cdot y + (\sin \psi \sin \gamma) \cdot z. \quad (8)$$

Normally, only two angles are required to fully describe an arbitrarily oriented plane. In this case, however, the third angle is required to allow for the arbitrarily oriented object when the rotational property of the Radon transform is presented. The intersection of the planes given by Equations (7) and (8) and the ellipsoid function of Equation (6) define the x-ray path intersection with the ellipsoid associated with point  $(r_o, t_o)$  on the detector plane. The points of intersection in terms of only the x coordinate are given by the quadratic equation

$$x^2 \left( \frac{1}{A^2} + \frac{R^2}{B^2} + \frac{T^2 P^2}{C^2} \right) + x \left( \frac{2P^2 S T}{C^2} - \frac{2QR}{B^2} \right) + \left( \frac{Q^2}{B^2} + \frac{P^2 S^2}{C^2} - 1 \right) = 0 \quad , \quad (9)$$

where

$$P = \left( \frac{b}{fb - ec} \right) \quad Q = \frac{1}{b^2} \left\{ t_o - \left( \frac{cb}{fb - ec} \right) \left( r_o - \frac{ct_o}{b} \right) \right\}$$

$$R = \left\{ \left( \frac{b}{fb - ec} \right) \left( \frac{ea}{b} - d \right) + a \right\} \quad S = \left( r_o - \frac{ct_o}{b} \right) \quad T = \left( \frac{ea}{b} - d \right)$$

and

$$\begin{aligned}
 a &= \cos \psi \cos \theta - \sin \psi \cos \gamma \sin \theta \\
 b &= \cos \psi \sin \theta + \sin \psi \cos \theta \cos \gamma \\
 c &= \sin \gamma \sin \psi \\
 d &= \sin \gamma \sin \theta \\
 e &= -\sin \gamma \cos \theta \\
 f &= \cos \gamma
 \end{aligned}$$

Thus the solution points are:

$$x_{1,2} = \frac{\frac{2QR}{B^2} - \frac{2P^2ST}{C^2} \pm \sqrt{\left(\frac{2QR}{B^2} - \frac{2P^2ST}{C^2}\right)^2 - 4 \left(\frac{1}{A^2} + \frac{R^2}{B^2} + \frac{T^2P^2}{C^2}\right) \left(\frac{Q^2}{B^2} + \frac{P^2S^2}{C^2}\right)}}{2 \left(\frac{1}{A^2} + \frac{R^2}{B^2} + \frac{T^2P^2}{C^2}\right)} \quad (10)$$

and the difference,

$$x_1 - x_2 = \frac{\sqrt{\left(\frac{2QR}{B^2} - \frac{2P^2ST}{C^2}\right)^2 - 4 \left(\frac{1}{A^2} + \frac{R^2}{B^2} + \frac{T^2P^2}{C^2}\right) \left(\frac{Q^2}{B^2} + \frac{P^2S^2}{C^2}\right)}}{\left(\frac{1}{A^2} + \frac{R^2}{B^2} + \frac{T^2P^2}{C^2}\right)} \quad (11)$$

defines the length of the path through the ellipsoid. Because we know the orientation of the x-ray path, we can write the distance of the x-ray inside the ellipsoid in terms of the orientation angles and the x coordinate difference.

$$d = \frac{x_1 - x_2}{\cos \gamma \cos \theta} \quad (12)$$

We may now account for arbitrary ellipsoid location and rotation through the translation and rotation properties of the Radon transform. These properties are given in Equations (13) and (14) for a shift of  $(x_o, y_o, z_o)$  and a rotation by three angles  $\theta$ ,  $\gamma$  and  $\psi$ .

$$\begin{aligned}
 \mathcal{R}[f(x-x_o, y-y_o, z-z_o)] &= \mathcal{E}_{\theta, \gamma, \psi}(t - x_o \cdot (\cos \psi \cos \theta - \sin \psi \cos \gamma \sin \theta - \sin \gamma \sin \theta) - \\
 &\quad y_o \cdot (\cos \psi \sin \theta + \sin \psi \cos \theta \cos \gamma + \sin \gamma \cos \theta), \quad (13) \\
 &\quad r - z_o \cdot (\cos \gamma - \sin \psi \sin \theta))
 \end{aligned}$$

$$\mathcal{R}[f_{\theta+\theta_o, \gamma+\gamma_o, \psi+\psi_o}(x, y, z)] = \mathcal{E}_{\theta+\theta_o, \gamma+\gamma_o, \psi+\psi_o}(t, r) \quad (14)$$

These properties are used in Equations (11) and (12) by making the substitutions for  $t$ ,  $r$ , and the angles,  $\theta$ ,  $\gamma$  and  $\psi$ , yielding the forward projection model for an arbitrarily

oriented and located ellipsoid. We must now make a transformation to account for the cone beam x-ray source. The transformation, given by Equations (15)-(18) transforms each cone-ray to some equivalent parallel source orientation to allow the same form of the expression for d to be used in the model. The variable D in the equations below is the perpendicular distance from the source to the detector.

$$\theta' = \theta + \tan^{-1} \frac{t_o}{D} \quad (15)$$

$$t'_o = D \cdot \sin \left( \tan^{-1} \frac{t_o}{D} \right) \quad (16)$$

$$\gamma' = \gamma + \tan^{-1} \left( \frac{r_o}{\sqrt{D^2 + t_o^2}} \right) \quad (17)$$

$$r'_o = \sin \left( \tan^{-1} \left( \frac{r_o}{\sqrt{D^2 + t_o^2}} \right) \right) \cdot \sqrt{D^2 + t_o^2} \quad (18)$$

With a forward model for the ellipsoidal projection, projection data can be used to solve for the unknown model parameters. An important assumption made here is that the measured projection data can be described by the model. Admittedly, not all volumetric flaws can be accurately modeled by an ellipsoid, however, the inversion technique will attempt to fit the best ellipsoid to the data and will give a measure of “goodness of fit” so that a parameter solution can be viewed with suspicion when appropriate. Theoretically, the model parameters can be uniquely determined from one projection and nine measurements on the detector. In practice, however, many more measurements and possibly more projections should be used to minimize effects of measurement errors and to improve the model fit.

We formulate this problem as a parameter estimation problem with a nonlinear model. There are well-known techniques available in the field of statistics to handle this problem, such as nonlinear least squares estimation and maximum likelihood estimation [7]. The problem is formulated as follows:

Let  $d_i$  represent the  $i$ th detector measurement at some known position  $(r_i, t_i)$ . Let  $g$  be the modeling function with unknown parameters. For  $n$  detector measurements, we have a nonlinear overdetermined system of  $n$  equations and nine unknowns.

$$\begin{aligned} d_1 &= g(r_1, t_1, \theta_1, \gamma_1, \psi_1; A, B, C, x_o, y_o, z_o, \theta_o, \gamma_o, \psi_o) \\ d_2 &= g(r_2, t_2, \theta_2, \gamma_2, \psi_2; A, B, C, x_o, y_o, z_o, \theta_o, \gamma_o, \psi_o) \\ &\vdots \\ d_9 &= g(r_9, t_9, \theta_9, \gamma_9, \psi_9; A, B, C, x_o, y_o, z_o, \theta_o, \gamma_o, \psi_o) \\ &\vdots \\ d_n &= g(r_n, t_n, \theta_n, \gamma_n, \psi_n; A, B, C, x_o, y_o, z_o, \theta_o, \gamma_o, \psi_o) \end{aligned}$$

We may now implement an estimation technique on this system. Work is currently under way on this implementation using a maximum likelihood estimator in conjunction with a

chi-square statistic for evaluation of the goodness of fit [5]. Simulated projection data is being used from an x-ray simulation program [6].

## CONCLUSION

The work presented in this paper is aimed at reconstructing flaw models rather than actual flaw distributions using a small number of projections and a simple experimental setup. We have presented the crack-like flaw reconstruction technique developed previously in terms of a linear model so that the method of total least squares could be applied as a parameter estimator. We have also presented the forward model for the ellipsoidal flaw model and preliminary ideas for the optimal estimation of the model parameters. The next step for this work is to test the technique using simulated data and to finally, evaluate its validity with experimental NDE data.

## ACKNOWLEDGEMENT

We thank Joe Gray for his useful discussions and advice on this work.

## REFERENCES

1. Wallingford, R. M. and Basart, J. P. in Review of Progress in Quantitative NDE. edited by D. O. Thompson and D. E. Chimenti, (Plenum Press, New York, 1989), Vol 8a, pp. 351-358.
2. Wallingford, R. M. and Basart, J. P., Twenty-Second Annual Asilomar Conference on Signals, Systems, and Computers. (IEEE Computer Society, Maple Press, 1989) pp. 68-72.
3. Golub, G. H. and Van Loan, C. F., SIAM J. Numer. Anal. Vol. 17, No. 6, pp. 883-893, December, 1980.
4. Branham, R. L., Computers in Physics. pp. 42-46, May/June, 1989.
5. Press, W. H., Flannery, B. P., Teukolsky, S. A. and Vetterling, W. T. Numerical Recipes in C: The Art of Scientific Computing. Sections 14.2, 14.4, 14.5. (Cambridge University Press, Cambridge, 1988).
6. Gray, J. N., Inanc, F. and Shull, B. E. in Review of Progress in Quantitative NDE, edited by D. O. Thompson and D. E. Chimenti, (Plenum Press, New York, 1989), Vol. 8a, pp. 345-350.
7. Fuller, W. A. Measurement Error Models, Sections 3.2, 3.3 (Wiley, New York, 1987).